



HAL
open science

Spatial distribution of trace elements in the soils of south-western France and identification of natural and anthropogenic sources

Lionel Savignan, Alexandre Lee, Alexandra Coynel, Stéphanie Jalabert, Stéphane Faucher, Gaetane Lespes, Philippe Chéry

► **To cite this version:**

Lionel Savignan, Alexandre Lee, Alexandra Coynel, Stéphanie Jalabert, Stéphane Faucher, et al.. Spatial distribution of trace elements in the soils of south-western France and identification of natural and anthropogenic sources. *CATENA*, 2021, 205, pp.105446. 10.1016/j.catena.2021.105446 . hal-03240150

HAL Id: hal-03240150

<https://hal.science/hal-03240150>

Submitted on 27 May 2021

HAL is a multi-disciplinary open access archive for the deposit and dissemination of scientific research documents, whether they are published or not. The documents may come from teaching and research institutions in France or abroad, or from public or private research centers.

L'archive ouverte pluridisciplinaire **HAL**, est destinée au dépôt et à la diffusion de documents scientifiques de niveau recherche, publiés ou non, émanant des établissements d'enseignement et de recherche français ou étrangers, des laboratoires publics ou privés.

Spatial distribution of trace elements in the soils of south-western France and identification of natural and anthropogenic sources

Lionel Savignan ^{a,c}, Alexandre Lee ^a, Alexandra Coynel ^b, Stéphanie Jalabert ^a, Stéphane Faucher ^c, Gaëtane Lespes ^{c*}, Philippe Chéry ^{a*}

^a Bordeaux Science Agro, EA 4592 Géoressources et environnement, 1 cours du Général De Gaulle, 33175 Gradignan, France

^b Université de Bordeaux, UMR EPOC CNRS 5085, 33615 Pessac, France

^c Université de Pau et des Pays de l'Adour / E2S UPPA, CNRS, Institut des Sciences Analytiques et de Physico-Chimie pour l'Environnement et les Matériaux (IPREM), UMR 5254, Helioparc, 2 avenue Pierre Angot, 64053 Pau Cedex 09, France

*corresponding authors : gaetane.lespes@univ-pau.fr; philippe.chery@agro-bordeaux.fr

Keywords: multivariate analysis, geostatistics, GIS, monitoring network

Abstract:

The contamination of soils by trace elements is a major concern for soil quality. This study is based on the analysis of 356 samples from the RMQS soil-monitoring network to establish the spatial distribution and origin of six trace elements (As, Cd, Cu, Cr, Ni, Pb) in soils of south-western region of France (area of 90,293 km²). An exploratory and multivariate statistical analysis, and geostatistics combined with a geographic information system (GIS) were used to identify and characterize any concentration anomalies in trace elements. For all the trace elements studied, the exploratory analysis shows that there are more anomalies in this region than in the rest of the country. Analysis of the semivariograms shows that the six elements are spatially auto correlated. The spatial structure of As highlights anisotropic behaviour with a direction that corresponds to the gold deposit and mining activities of the region. This indicates a dual origin anthropogenic and geogenic for As. The correlation between Cd and inherent features of calcareous soil (pH, CaCO₃ and cation exchange capacity) suggest a mainly geogenic origin for this element; Cd origin is confirmed by its spatial distribution associated with the Jurassic limestone bedrock. The correlations between Cr, Ni and clays highlight a geogenic origin for these elements, as weathered parent material rich in clays is also rich in Cr and Ni. The high Cu concentrations are of anthropogenic origin, linked to viticulture and the spreading of Bordeaux mixture as a fungicide. Locally high Pb concentrations are associated with mining activities and automobile emissions in large cities in the region.

33 **1. Introduction**

34 The contamination of soils by trace elements (TE) are of major concern with regard to
35 potential plant growth and food health issues due to high concentrations of metals and/or
36 metalloids in soils (McLaughlin et al., 1999). TEs are naturally present in soils. Their natural
37 concentrations depend not only on the physical and chemical weathering of the parent rock
38 and on pedogenesis, but also on the transport of materials of colluvial, fluvial and even wind
39 origin; they also depend on their mobility, which is different from one element to another
40 depending on the physico-chemical parameters (e.g. pH, Eh,...). TE concentrations in soils
41 can be modified significantly by anthropogenic pressures of urban, industrial, mining and
42 agricultural origin (Belon et al., 2012). Thus, anthropogenic inputs can exceed inputs from
43 natural cycles and the assimilative capacity of soils. Due to natural variability and widespread
44 and diffuse anthropogenic inputs, it is common for the spatial distribution of TE
45 concentrations in soils to be not random. That is, observations that are close to each other tend
46 to resemble each other more than those that are further away. It is therefore common for TE
47 concentrations in soil topsoil to be spatially correlated. In this case, geostatistical
48 spatialisation methods may prove useful in assessing spatial variability and sources of trace
49 elements in soils (Atteia et al., 1994; Facchinelli et al., 2001). The combined use of
50 Geographic Information System (GIS) and tools such as multivariate analysis and exploratory
51 data analysis can help determine the origin of trace elements (Facchinelli et al., 2001; Hou et
52 al., 2017; Saby et al., 2009).

53 The spatial distribution of trace elements over large national or continental areas has been
54 studied for a long time in order to establish geochemical baseline (Chen et al., 1991; McGrath
55 and Loveland, 1992; Salminen, 2005; Shacklette and Boerngen, 1984). More recently,
56 national and continental soil monitoring networks have been set up in Europe to determine
57 soil qualities (including TE content) and monitor their temporal and spatial changes in TE

58 levels (Morvan et al., 2008). In Europe, the LUCAS survey was launched to build a consistent
59 spatial database of the soil cover over the EU (Orgiazzi et al., 2018). In France, the national
60 monitoring network (Réseau de Mesures de la Qualité des Sols, RMQS), was designed to
61 assess the concentration of 11 TE (As, Cd, Cr, Cu, Hg, Mo, Ni, Pb, Tl, Zn), among other
62 objectives (Arrouays et al., 2003). This network has enabled the spatial distribution of trace
63 elements in soils to be established at a national scale (Marchant et al., 2017, 2010; Saby et al.,
64 2011). We propose to use this network at a regional scale, over the southwestern region of
65 France (SWF), which covers a surface of 90,293 km² similar to European countries such as
66 Belgium, Austria or mainland Portugal.

67 The main objective of this study was to determine the spatial distribution and origin of TE in
68 the soils of SWF; this in order to produce knowledge that can be used to support regional
69 territorial decisions. Indeed, in this region the agricultural productions are numerous and
70 varied, and they are subject to many risks of contamination by TE, either of geogenic origin
71 or of anthropogenic origin. To achieve this objective, we (i) used the national RMQS
72 program, (ii) determined the reference concentrations of selected TE in the SWF soils, (iii)
73 determined their spatial variability in the region using geostatistics, and then, (iv) highlighted
74 anomalies and their origins using statistical and geostatistical tools and the crossing of
75 geographic databases with spatial distributions. The trace elements were selected according to
76 the risk of contamination for the production of food biomass. Therefore, the following
77 elements were considered:

78 - As, ubiquitous metalloid, the use of which as a pesticide and the presence in mineral
79 fertilizers have led to severe pollution of soil and water, causing accumulations in the food
80 chain. This element presents a high health risk because it is toxic in all its inorganic forms
81 (Mandal, 2002).

82 - Cd, found in phosphate fertilizers and manure spread on soils (Belon et al., 2012). This
83 element presents a high health risk as a carcinogen (IARC, 1993).

84 - Cu, widely used in vineyard areas and present in the manure spread. This element affects
85 the microbial life of the soil due to its biocidal action (Ranjard et al., 2008).

86 - Cr, resulting from industrial activities (e.g. effluents from tanneries) and which can be
87 found in soils due to irrigation. It is also brought into the soil by manure spreading. This
88 element presents a health risk because it is carcinogenic in its hexavalent form.

89 - Ni, brought into the soil by manure spreading, due to mining activities or as a by-product
90 associated with other types of pollutants such as PAHs (Barcan and Kovnatsky, 1998;
91 Belon et al., 2012; Zehetner et al., 2009). This element is not very phytotoxic and presents
92 less health risk than the elements above. However, anthropogenic contributions to soils can
93 be significant (Rooney et al., 2007).

94 - Pb, from mining, industrial and road traffic emissions. Its accumulation in the food chain
95 induces a significant health risk (lead poisoning).

96 Complementarily, Fe, Mn and Al were also considered to be major elements involved in
97 different types of pedogenesis. Their concentrations were compared with the
98 concentrations of the selected trace elements to highlight correlations and deduce the
99 origin of these trace elements.

100 **2. Materials and methods**

101 *2.1 Study area*

102 The area includes the Nouvelle Aquitaine region, which is the largest agricultural region in
103 France (39,000 km² of usable agricultural area) and the department of Gers. The agricultural
104 production of this area is varied (field crops, livestock farming, viticulture and arboriculture).

105 The area also includes large forest areas (28,000 km²) with particularly the Landes de
106 Gascognes massif, the largest forest surface of Western Europe, located to the south-west of
107 the region (Figure 1A). The study area is inhabited by 6.1 million people, including
108 1.2 million within the urban area of Bordeaux (Figure 1A).

109 The soils of this region are described by three major soil systems depending on the nature of
110 the parent material and the climate (Figure 1B): (i) the soils derived from materials of
111 sedimentary origin among which there are calcareous alkaline soils (Cambisol, Rendzina),
112 acidic black sandy soils of the Landes (Podzol), and soils resulting from recent alluvial
113 deposits (Fluvisol, Histosol, Gleysol) (Figure 1B); (ii) the Cambisols of the north-western part
114 of the region are soils derived from materials of granite or metamorphic origin (Figure 1C),
115 and (iii) in the south of the region, near the Pyrenees mountain range, the soils resulting from
116 folded geological formations on which limestone Cambisols and Lithosols have formed.

117 2.2 *Sampling plan*

118 The RMQS network grid in SWF corresponds to 356 sampling sites, sampled between 2000
119 and 2009. The locations of the sites were chosen if possible at the centre of each 16x16 km
120 cell (Figure S1), or otherwise in a radius of 1 km around (Jolivet et al., 2006). The types of
121 land use are also listed as well as the crop management technique used on each plot concerned
122 by the sampling. On each site, soil samples were collected according to the protocol of the
123 RMQS network manual (Jolivet et al., 2006): 25 individual cores in the topsoil (0-30 cm to
124 +/- 5 cm depending on the thickness of the first organo-mineral horizon) using a stratified
125 random sampling plan in an area of 20 × 20 m (see Figure S1). For each site, the cores were
126 mixed to obtain composite soil samples. The organic horizon was discarded from composite
127 soil samples. A pit was dug near (5 m) and to the south of the sampling area in order to
128 describe the soil profile and to perform specific measurements (bulk density, coarse elements,

129 etc.). This protocol was used for all studies based on the RMQS (Marchant et al., 2017; Saby
130 et al., 2011, 2006, 2009).

131 2.3 *Physico-chemical analyses*

132 Soil samples were air dried and sieved at 2 mm before analysis (AFNOR, 1994a). The
133 granulometry (clays, coarse and fine silts, coarse and fine sands) was determined without
134 decarbonation by Robinson pipette (AFNOR, 2003). The pH was measured after mixing the
135 soil with deionised water (soil /water ratio 1/5, v/v) (AFNOR, 1994b). The cation exchange
136 capacity (CEC) was determined by extracting cations (Ca^{2+} , Mg^{2+} , K^+ , Na^+) with
137 cobaltihexamine chloride (AFNOR, 1999). CaCO_3 content was determined by treatment with
138 HCl (12%), then the volume of carbon dioxide produced is measured with a Scheibler
139 apparatus (AFNOR, 1995a). The total organic carbon and total nitrogen contents were
140 determined by dry combustion after decarbonation (AFNOR, 1995b). The total concentrations
141 of trace (As, Cd, Cr, Cu, Ni and Pb) and major elements (Al, Fe, Mn) were determined, after
142 digestion of samples with a mixture of HF (49 %) / HClO_4 (69 %) (5 / 1.5 mL), by inductively
143 coupled plasma mass spectrometry for trace elements, and by inductively coupled plasma
144 atomic emission spectrometry for major elements (AFNOR, 2001). These analyses were
145 carried out by the Soils Analysis Laboratory of INRA in Arras (France), accredited by the
146 French authorities for the analysis of soils and sludges.

147 2.4 *Statistical analyses*

148 The exploratory data analysis technique (Tukey, 1977) was used to obtain the reference total
149 concentrations (median, minimum, maximum) of the studied TE. This method is based on
150 nonparametric statistics (i.e. which do not depend on a probability law) and enables robust
151 indicators (medians, quartiles) of the data set to be obtained (Reimann et al., 2005). The limit
152 values, called lower whisker and upper whisker, are calculated with the following formulas:

153 (1) Lower whisker = $Q1 - 1.5 \times IQR$

154 (2) Upper whisker = $Q3 + 1.5 \times IQR$

155 where Q1 is the first quartile, Q3 the third quartile and IQR the interquartile range (Q3–Q1).
156 Extreme values are defined as being outside the limit values. For the statistical analyses of
157 this study, the concentration values below the limit of quantification were replaced
158 numerically by half of the value of the limit of quantification (Farnham et al., 2002).
159 Cartograms of the study area were generated to illustrate the distribution of concentrations of
160 studied trace elements relating to each sampling site with a classification by quartiles.

161 Principal component analysis (PCA) enables the correlations (or their absence) between
162 selected variables to be highlighted. When PCA was applied to TE concentrations in soils, it
163 provided answers regarding their sources (Facchinelli et al., 2001). A PCA was therefore
164 carried out by taking as variables the concentrations of the 6 selected trace elements (As, Cd,
165 Cr, Cu Ni, Pb) and pedologic variables: the concentrations of the major elements (Fe, Mn and
166 Al), granulometry (5 fractions), pH, organic carbon and total nitrogen. The data analysis was
167 carried out with R software version 3.5.1 (R Core Team, 2019) and for the calculation of the
168 PCA the FactoMineR library was used (Lê et al., 2008).

169 2.5 *Spatial and geostatistical analysis*

170 The geostatistical treatments were carried out from the study of semivariograms.
171 Semivariograms are used to describe the structure (organization and regularity of the variable
172 in the space considered) and the spatial variability of the data. They estimate the semivariance
173 $\gamma(h)$ of a variable measured at two points distant from h , and thus estimate the importance of
174 the link (i.e. the degree of continuity) between these points for this variable (autocorrelation).
175 Semivariograms show how the information between two measurement points of this variable
176 degrades as the distance increases. The evolution of information is therefore represented by an

177 increasing function up to a sill defined by the maximum interpolation distance. This distance
 178 also corresponds to the distance from which two consecutive values are independent. The
 179 equation of the semivariogram is:

$$180 \quad (3) \quad \gamma(h) = \frac{1}{2N(h)} \sum_{i=1}^{N(h)} \left\{ [Z(x_i + h) - Z(x_i)]^2 \right\}$$

181 where $\gamma(h)$ is the semivariance, $N(h)$ the number of point pairs, h the distance between 2
 182 points, $Z(x_i)$ is the concentration of the element at location x_i . The experimental
 183 semivariograms of the various variables considered were calculated for an interpoint distance
 184 of 16 km (which corresponds to the size of the cell of the RMQS grid). They were then
 185 empirically fitted by a mathematical function comprising a sill. The fitting enabled
 186 information on the spatial structure of the variable to be obtained thanks to the following
 187 parameters: the nugget (value of the y-intercept; represents the part of variability lower than
 188 the sampling interval), the sill, and the range (distance from which the sill is reached and
 189 beyond which there is no longer any autocorrelation). The fitting of the semivariogram by an
 190 experimental empirical mathematical model was performed by iterative least squares
 191 weighting, minimizing the following expression:

$$192 \quad (4) \quad \sum_{j=1}^n N(h) (\hat{\gamma}(\bar{h}_j) - \gamma(\bar{h}_j))^2$$

193 Where $\gamma(\bar{h}_j)$ is the experimental value of the semivariance, and $\hat{\gamma}(\bar{h}_j)$ is the modeled value
 194 of the semivariance. The geostatistical calculations were carried out with the gstat library and
 195 the R software (Pebesma, 2004). The ratio between the nugget and the total variance
 196 (hereinafter called nugget/variance ratio) was calculated in order to have a relative assessment
 197 of the nugget effect (expressed in %), which is more explicit than the absolute value and
 198 enables comparisons. The anisotropy was studied from a semivariance map with two direction
 199 axes for each trace element considered. This map enables a possible preferential direction in

200 the variation of the semivariance to be highlighted. Directional semivariograms were modeled
201 with an angle tolerance of 45° to obtain a sufficient number of point pairs.

202 From the semivariogram modeling parameters (nugget, sill, range), ordinary kriging was
203 applied to produce spatial distribution maps of TE concentrations. The maps were generated
204 using ArcGIS version 10.1 software (Esri, 2012). Several databases were used to determine
205 the origin of the trace elements: SIG Mines France for the location of old mines and ore
206 deposits (BRGM, 2007), and BD-CHARM geological maps (scale 1/50000) for parent
207 material (BRGM, 2005). Soil occupation was described directly from the RMQS sites. All
208 these data were crossed with the distribution maps of the trace elements in order to highlight
209 the possible sources of contamination and the modes of transfer of these elements to the soil.

210

211 **3. Results and discussion**

212 *3.1 Descriptive statistics*

213 The preliminary observation of the statistical variables enables any particularities of the
214 studied dataset to be identified, and thus a better guided statistical analysis strategy to be
215 carried out.

216 Table 1 presents the statistical characteristics of the concentrations of the trace elements
217 studied. The regional and national median values are close, which seems to show the
218 homogeneity of the concentrations in SWF compared to the whole of France. In more detail,
219 Figure 2 shows the maps of TE concentrations. The distribution of concentrations does not
220 appear to be regular. In particular, on the one hand, the Landes massif (around 15 % of the
221 soil samples) shows very low concentrations of the trace elements studied. On the other hand,
222 by defining the whiskers as anomaly thresholds, there are more sites with anomalous TE
223 concentrations (As, Cu, Pb) in the SWF according to the national threshold than according to

224 the regional threshold (Table 1). Therefore, there would be geogenic anomalies and/or
225 regional contaminations for As, Cu, and Pb while anomalies would be less substantial for Cd,
226 Cr and Ni. All of these observations highlight the interest of carrying out a more in-depth
227 spatial study in order in particular to locate these anomalies and identify their origin. In
228 addition, Table 2 presents the statistical characteristics of the soil variables considered in this
229 study. For all these variables, large amplitude of values is observed for the 356 soils sampled.
230 This is particularly the case for the concentrations of clay, pH, CaCO₃, organic matter, Fe and
231 Al. Special attention was therefore granted to these variables, known to drive the TE
232 variability.

233 *3.2 Multivariate analysis: first approach to the origin of the trace elements*

234 In order to complete the previous observations by considering all the information points of the
235 datasets, a multivariate analysis was carried out by PCA. Figure 3 presents, by decreasing
236 contributions, the 6 components (or dimensions) that explain 79% of the total variance. The
237 main contributions of the variables to the components are as follows (Table S1). The
238 concentrations of clay, coarse sand, Al, Fe, Cr, Ni, Cd and CEC for the principal component 1
239 (PC1); organic carbon, total nitrogen, pH and CaCO₃ for principal component 2 (PC2); coarse
240 silt, CaCO₃, CEC, pH and Cd for PC3; As, silt, carbon and nitrogen for PC4; fine sand, Pb
241 and Cu concentration for PC5; fine sand and Cu for PC6. The negative correlation between
242 coarse sands and TE concentrations suggests that soils with a high percentage of coarse sand
243 are rather poor in trace elements. This is confirmed by the lowest TE concentrations that are
244 located in the Landes forest, with mainly sandy soils of recent geological formation (<1 Ma),
245 and with an acidic pH which causes the solubilisation of the elements (Righi and Wilbert,
246 1984). In addition, sand has a lower specific surface, which does not promote the adsorption
247 of elements (Daskalakis and O'Connor, 1995; Schiff and Weisberg, 1999).

248 It can be also observed:

249 - In Figure 3A, the concentrations of Cr, Fe, Ni and the clay content correlate positively.

250 This suggests a rather geogenic origin of Cr and Ni. Indeed, the materials resulting from
251 the degradation of rocks rich in Cr and Ni are also rich in clays. Thus Cr, Ni and clays
252 would remain bound after the weathering of these rocks and transfer to the soil (Cheng et
253 al., 2011; Kierczak et al., 2007). This was observed in a previous study (ASPITET) on
254 trace elements in soils in France (Baize, 1997).

255 - In Figure 3B, Cd concentrations, CaCO₃, pH and CEC also correlate positively. In the
256 study region, soils with high CaCO₃ content, pH, and CEC are limestone soils. The
257 association between Cd and certain carbonate minerals could therefore explain this
258 correlation, as it was already observed in natural environments (Chada et al., 2005; Martin-
259 Garin et al., 2002). This association is the result of the carbonate dissolution reaction,
260 where Cd²⁺ would replace Ca²⁺ to form CaCO₃-CdCO₃ or CdCO₃ (Papadopoulos and
261 Rowell, 1988). The introduction of Cd into soils by amendments based on calcium
262 carbonates and phosphate fertilizers is also a possible source of Cd in soils (Senesil et al.,
263 1999).

264 - In Figure 3C and 3D, no correlation could be noted for the concentrations of As, Cu and Pb
265 with the other variables in PCs that explain a low amount of the total variance. This
266 suggests rather a predominantly anthropogenic origin of these elements.

267 3.3 *Spatial and geostatistical analysis: factors influencing spatial distribution*

268 In order to bring a spatial dimension to the analysis of TE concentrations, their
269 semivariograms were calculated and are shown in Figure 4. These semivariograms were
270 obtained using equation (3) and are given with their associated parameters (especially nugget
271 effect, range and nugget/variance ratio; shown in the column to the right of each

272 semivariogram). To complete, Figure 5 presents the thematic maps of the TE concentrations
273 predicted by ordinary kriging (using the parameters of the semivariograms of each trace
274 element). Geographical information on land use, mining activities, parent material and
275 mineral deposits are overlaid on concentration maps. Thus, all of the information obtained and
276 used can be viewed together.

277 All semivariograms (Figure 4) are bounded. This means that the spatial structures of the TE
278 concentrations are included in the regional study area. In other words, the concentrations of a
279 given trace element spatially depend on the range scale, which varies from 86 to 154 km
280 depending on the element considered. For all variograms, the nugget/variance ratios are
281 between 40 and 80 %. These values are partly induced by the size of the sampling grid
282 (16x16 km). This indicates that it was not possible to detect significant local variations.

283 The directional analysis of the semivariograms revealed an anisotropy for As only, as
284 illustrated in Figure 6. The spatial structure of this element differs according to the direction
285 considered (as illustrated in the Figure S2 drawn in orthogonal directions north–south and
286 east–west). In particular, in the north–south direction (0°) the semivariogram is circular,
287 without nugget effect and with a very short range (24 km). In the northeast–east direction
288 (60°) the semivariogram is spherical, with a strong nugget effect and a range close to that of
289 the omnidirectional semivariogram (115 km). The direction of the directional semivariogram
290 of As (60°) points to the gold mining zones located to the north and northeast of the region. In
291 this area, the deposits consist of quartz veins containing native As and Au-As-S minerals
292 resulting from hydrothermal processes in granitic and metamorphic rocks (gneiss).
293 Consequently, As can be considered as a geochemical tracer of Au in this area (Bossy, 2010;
294 de Gramont and Braux, 1990). In addition, gold mining from the Gallic period until the end of
295 the 1960s led to the contamination of the Isle watershed by mining residues and therefore in
296 particular by As (Cauuet, 1991; Courtin-Nomade et al., 2002; Grosbois et al., 2007).

297 Cd does not exhibit a particularly high nugget/variance ratio (60 %) but has a greater range
298 compared to the majority of trace elements studied (> 135 km). This suggests a distribution of
299 Cd due to a single and extended source. In fact, and given that Cd is positively correlated with
300 pH and CEC, the presence of Cd would correspond to the presence of limestone substrates
301 (parent material and/or coarse fragments), therefore to a mainly geogenic origin. This is in
302 agreement with the work by Atteia et al. (1995) in the Swiss Jura and Baize et al. (1999) in
303 Bourgogne, where the Cd concentration was correlated with Jurassic age limestone. This
304 interpretation is also relevant insofar as such limestone soils of the same geological age are
305 present in the SWF, in particular in the departments of Dordogne and Charentes, i.e. in the
306 centre and northwest of the region, respectively (Figure 5). Very high Cd concentrations were
307 also found at two sites located on the alluvial deposits of the Garonne river (Figure 5). These
308 anomalies can be explained by the historical cadmium contamination of the Lot-Garonne
309 hydrological continuum that carries suspended matter directly from the Decazeville industrial
310 basin following the extraction and processing of ores rich in Zn and Cd or indirectly due to
311 the remobilization of sediments accumulated behind the dams of the Lot river (Audry et al.,
312 2004; Coynel et al., 2009, 2007; Dabrin et al., 2009; Pougnet et al., 2019).

313 Cu has the highest nugget/variance ratio (81 %) and a large range (112 km), which can be
314 explained by the anthropogenic input of this element in the vineyards of the region (Figure 5).
315 Indeed, Cu has been used in viticulture in a mixture of copper sulphate and lime (Bordeaux
316 mixture) to fight against downy mildew (*Peronospora viticola*) since the end of the 19th
317 century (Ayres, 2004). This cultivation practice has led to diffuse soil contamination in
318 French wine-growing areas and in particular in Gironde, as mentioned in previous studies
319 (Baize et al., 2006; El Hadri et al., 2012). However, this contribution remains very
320 heterogeneous depending on the vine management technique chosen by the winegrowers as
321 well as the variability of the fungal pressure.

322 Cr and Ni have the lowest nugget/variance ratios (41 and 44% respectively). Less spatial
323 variability than for the other trace elements therefore appears for distances <16 km. This
324 suggests that the distribution of these two elements is mainly natural. This hypothesis would
325 be supported on the one hand by the fact that Cr and Ni are known to be not very mobile in
326 soils. On the other hand, these elements are usually found strongly adsorbed on the mineral
327 components of the soil such as calcite, illite and montmorillonite (Businelli et al., 2004;
328 Hickey and Kittrick, 1984; Mamindy-Pajany et al., 2013; Navarro-Pedreño et al., 2003). This
329 is relevant given the positive correlation with clays found above. The Cr and Ni
330 concentrations in SWF soils therefore appear to depend on the underlying bedrock, with high
331 concentrations being found in soils from Jurassic and Cretaceous rocks (Figure 5). This
332 dependence was already observed for the RMQS network at the national level (GIS Sol,
333 2011). Similar results were found by the FOREGS program on French soils (Salpeteur and
334 Maldan, 2011). If anthropogenic contaminations are possible, for example by spreading
335 sludge or due to industrial discharges, then they are probably very localised and therefore not
336 detected in the RMQS grid.

337 Pb has a high nugget/variance ratio (79%), with a lower range than the other elements (85
338 km). Its regional spatial distribution shows high concentrations in the north and northeast of
339 the region, with spots near large urban areas (Bordeaux, Bayonne, etc.) (Figure 5).
340 Concentrations in the northeast of the region are believed to be mainly of mining origin
341 (Courtin-Nomade et al., 2002; de Gramont and Braux, 1990). The spots close to large cities
342 are likely due to the density of traffic and the use of leaded gasoline until 2000 in France. The
343 work by Saby et al. (2006) led to a similar observation around the Paris urban area. Several Pb
344 spots are also found in forests and Pyrenean passes. They could come from hunting activities,
345 Pb shot being disseminated in soil samples (Mellor and McCartney, 1994; Tsuji and
346 Karagatzides, 1998).

347 3.4. *Statistical approaches: representativeness and limits*

348 The relatively high nugget/variance ratios obtained with semivariograms indicate that local
349 variations of TE concentrations cannot be detected by the 16x16 km grid. In other words, local
350 “hot spots” of TE concentrations may not be detected. Therefore, the issue of the
351 representativeness of the study on a regional scale could be raised. An analysis of the
352 representativeness of the different grid sizes (32x32, 16x16, 8x8 km) to design the RMQS
353 network was carried out (Arrouays et al., 2001). The analysis was based on the pair: soil type
354 – soil use pair. Results showed that with a 16x16 km grid, only 2.5% of the pairs are not
355 represented. In the SWF, the unrepresented part corresponds to small areas of vineyards and
356 orchards, which could have a significant input of TE. Targeted densification of the grid (e.g.
357 8x8 km) would help to better characterize these areas. However, this would also greatly
358 increase the number of sampling sites and consequently the implementation cost of the
359 network and the duration of the sampling.

360 In the present work we used upper whiskers as a first approach to detect anomalies in the TE
361 distribution. This simple approach, using descriptive statistics, has been widely used in
362 geochemical studies, including other studies based on the RMQS dataset (Redon et al., 2013;
363 Saby et al., 2009; Villanneau et al., 2008). However, it needs to be completed from other
364 approaches to discriminate between geogenic and anthropogenic anomalies. Saby et al. (2009)
365 determined the spatial patterns of TE over the whole of France with a spatially constrained
366 multivariate analysis method. The authors also identified the geogenic origin of Cd associated
367 with Jurassic limestone and the anthropogenic origin of Cu associated with the vineyard. At a
368 regional scale, Redon et al. (2013) combined the soil classification between calcareous and
369 non-calcareous soils, with several statistical methods (upper whiskers, enrichment factor,
370 PCA, linear regression) over the former Midi-Pyrénées region, adjacent to our study area. The
371 authors obtained similar results to ours, with Cu anomalies associated with the vineyard, but

372 found Cd and Pb contamination in grazing land suggesting sources from organic fertilization.
373 Finally, in the present work, we combined geostatistics and GIS that had the advantage of
374 producing intuitive maps with both TE concentrations anomalies and their associated sources.

375 **4. Conclusion**

376 The spatial distribution and variability of As, Cd, Cu, Cr, Ni, Pb for the south-western region
377 of France could be determined on the basis of the RMQS systematic sampling grid. The
378 regional median concentrations of these elements are close to the national values. However,
379 regional anomalous concentrations were highlighted by comparing with regional and national
380 whiskers taken as threshold values of anomaly and possible contamination. The origins of
381 these trace elements in SWF soils were identified combining cartographic and geostatistical
382 methods. Thus, As has a dual origin geogenic and anthropogenic, from gold deposit and
383 mining activities. Cu and Pb have anthropogenic origins, either linked to a main activity like
384 viticulture (Cu), or consecutive to several activities, mining, hunting and automobile traffic
385 (Pb). Cd, Cr and Ni are mainly of geogenic origin at the regional scale. In most cases,
386 contaminated areas are well demarcated. The Landes massif, with mostly sandy soils, contains
387 little content of trace elements.

388 The investigation approach used, combining systematic monitoring network and geostatistical
389 method, has thus shown its capability to detect contaminations in trace elements and to
390 identify their origins on a regional scale. This is possible despite a relatively large grid (16x16
391 km). This approach could therefore be transposable to countries with comparable surface
392 areas. Systematic soil monitoring networks have a dual interest: on the one hand, the data
393 acquired relating to soil quality can be used as a support element for national and regional
394 territorial decisions. This may concern environmental protection, agroecological transition or
395 food safety. On the other hand, these databases could be extended to other TE, not only those

396 monitored in the RMQS network but also to TE barely or not yet taken into account.
397 Emerging contaminations in the soil could then be identified. This would help to support
398 public decisions for the reduction and anticipation of pollution. This second point is
399 particularly important given the development of new technologies leading to an increasing use
400 of new elements (Alonso et al., 2012). These include the use of catalytic converters containing
401 platinoids (Pd, Pt, Rh), smartphones containing rare metals (such as Nd or Y) or MRI contrast
402 agents containing Gd (Lerat-Hardy et al., 2019; Schäfer et al., 1998). Finally, this type of
403 network could also enable changes in soil quality to be monitored by the early detection of
404 degradation that might be expected or not. A new campaign of soil sampling is ongoing for
405 the RMQS network.

406 **Acknowledgments**

407 This study was supported by a French Scientific Group of Interest on soils: the “GIS Sol”,
408 (involving the Ministry for an Ecological and Solidary Transition (MTES), the French
409 Ministry of Agriculture (MAA), the French Agency for Energy and Environment (ADEME),
410 the French Research Institute for Development (IRD), the French National Institute of
411 Geographic and Forest Information (IGN), the National Institute for Agronomic Research
412 (INRAE)) and Bordeaux Sciences Agro. Thanks are expressed to Claudy Jolivet, Céline Ratié
413 and Line Boulonne of unit INRAE US1106 InfoSol. We thank the three anonymous reviewers
414 for their comments that helped to improve this article.

415

416 **References**

- 417 AFNOR, 2003. NF X31-107. Qualité du sol. Détermination de la distribution granulométrique
418 des particules du sol. Méthode à la pipette.
- 419 AFNOR, 2001. NF ISO 14869-1. Qualité du sol. Mise en solution pour la détermination des
420 teneurs élémentaires totales. Partie 1: Mise en solution par l'acide fluorhydrique et l'acide
421 perchlorique.
- 422 AFNOR, 1999. NF X31-130. Qualité des sols. Méthodes chimiques. Détermination de la
423 capacité d'échange cationique (CEC) et des cations extractibles.
- 424 AFNOR, 1995a. NF ISO 10693. Qualité du sol. Détermination de la teneur en carbonate.
425 Méthode volumétrique.
- 426 AFNOR, 1995b. NF ISO 10694. Qualité du sol. Dosage du carbone organique et du carbone
427 total après combustion sèche (analyse élémentaire).
- 428 AFNOR, 1994a. NF ISO 11464. Qualité du sol. Prétraitement des échantillons pour analyses
429 physico-chimiques.
- 430 AFNOR, 1994b. ISO 10390. Qualité du sol. détermination du pH.
- 431 Alonso, E., Sherman, A.M., Wallington, T.J., Everson, M.P., Field, F.R., Roth, R., Kirchain,
432 R.E., 2012. Evaluating Rare Earth Element Availability: A Case with Revolutionary Demand
433 from Clean Technologies. *Environ. Sci. Technol.* 46, 3406–3414.
434 <https://doi.org/10.1021/es203518d>
- 435 Arrouays, D., Jolivet, C., Boulonne, L., Bodineau, G., Ratié, C., Saby, N., Grolleau, E., 2003.
436 Le réseau de mesures de la qualité des sols (RMQS) de France. *Etude Gest. Sols* 10, 241–250.
- 437 Arrouays, D., Thorette, J., Daroussin, J., 2001. Analyse de représentativité de différentes
438 configurations d'un réseau de sites de surveillance des sols. *Etude Gest. Sols* 8, 7–17.
- 439 Atteia, O., Dubois, J.-P., Webster, R., 1994. Geostatistical analysis of soil contamination in
440 the Swiss Jura. *Environ. Pollut.* 86, 315–327. [https://doi.org/10.1016/0269-7491\(94\)90172-4](https://doi.org/10.1016/0269-7491(94)90172-4)
- 441 Atteia, O., Thélin, Ph., Pfeifer, H.R., Dubois, J.P., Hunziker, J.C., 1995. A search for the
442 origin of cadmium in the soil of the Swiss Jura. *Geoderma* 68, 149–172.
443 [https://doi.org/10.1016/0016-7061\(95\)00037-O](https://doi.org/10.1016/0016-7061(95)00037-O)
- 444 Audry, S., Blanc, G., Schäfer, J., 2004. Cadmium transport in the Lot–Garonne River system
445 (France) – temporal variability and a model for flux estimation. *Sci. Total Environ.* 319, 197–
446 213. [https://doi.org/10.1016/S0048-9697\(03\)00405-4](https://doi.org/10.1016/S0048-9697(03)00405-4)
- 447 Ayres, P.G., 2004. Alexis Millardet: Frances forgotten mycologist. *Mycologist* 18, 23–26.
448 <https://doi.org/10.1017/S0269915X04001090>
- 449 Baize, D., 1997. Teneurs totales en éléments traces métalliques dans les sols (France):
450 Références et stratégies d'interprétation. Programme ASPITET, Un point sur. INRA, Paris.
- 451 Baize, D., Deslais, W., Gaiffe, M., 1999. Anomalies naturelles en cadmium dans les sols de
452 France. *Etude Gest. Sols* 2, 85–104.
- 453 Baize, D., Saby, N., Walter, C., 2006. Le cuivre extrait à l'EDTA dans les sols de France.
454 *Etude Gest. Sols* 13, 259–268.

455 Barcan, V., Kovnatsky, E., 1998. Soil Surface Geochemical Anomaly Around the Copper-
456 Nickel Metallurgical Smelter. *Water. Air. Soil Pollut.* 103, 197–218.
457 <https://doi.org/10.1023/A:1004930316648>

458 Belon, E., Boisson, M., Deportes, I.Z., Eglin, T.K., Feix, I., Bispo, A.O., Galsomies, L.,
459 Leblond, S., Guellier, C.R., 2012. An inventory of trace elements inputs to French agricultural
460 soils. *Sci. Total Environ.* 439, 87–95. <https://doi.org/10.1016/j.scitotenv.2012.09.011>

461 Bossy, A., 2010. Origines de l'arsenic dans les eaux, sols et sédiments du district aurifère de
462 St-Yrieix-la-Perche (Limousin, France) : contribution du lessivage des phases porteuses
463 d'arsenic. Université de Limoges, Limoges.

464 BRGM, 2007. SIG Mines France [WWW Document]. URL
465 <http://sigminesfrance.brgm.fr/index.asp> (accessed 4.24.18).

466 BRGM, 2005. BD-CHARM : Carte géologique de France à 1/50000 au format numérique
467 vecteur issue de la numérisation de la carte imprimée.

468 Businelli, D., Casciari, F., Gigliotti, G., 2004. Sorption mechanisms determining Ni(II)
469 retention by a calcareous soil. *Soil Sci.* 169, 355–362.
470 <https://doi.org/10.1097/01.ss.0000128015.92396.56>

471 Cauuet, B., 1991. L'exploitation de l'or en Limousin, des Gaulois aux Gallo-Romains. *Ann.*
472 *Midi* 103, 149–181. <https://doi.org/10.3406/anami.1991.2292>

473 Chada, V.G.R., Hausner, D.B., Strongin, D.R., Rouff, A.A., Reeder, R.J., 2005. Divalent Cd
474 and Pb uptake on calcite {101⁻⁴} cleavage faces: An XPS and AFM study. *J. Colloid*
475 *Interface Sci.* 288, 350–360. <https://doi.org/10.1016/j.jcis.2005.03.018>

476 Chen, J., Wei, F., Zheng, C., Wu, Y., Adriano, D.C., 1991. Background concentrations of
477 elements in soils of China. *Water Air Soil Pollut* 57–58, 699–712.
478 <https://doi.org/10.1007/BF00282934>

479 Cheng, C.-H., Jien, S.-H., Iizuka, Y., Tsai, H., Chang, Y.-H., Hseu, Z.-Y., 2011. Pedogenic
480 Chromium and Nickel Partitioning in Serpentine Soils along a Toposequence. *Soil Sci. Soc.*
481 *Am. J.* 75, 659–668. <https://doi.org/10.2136/sssaj2010.0007>

482 Courtin-Nomade, A., Neel, C., Bril, H., Davranche, M., 2002. Trapping and mobilisation of
483 arsenic and lead in former mine tailings –Environmental conditions effects. *Bull. Soc. Geol.*
484 *Fr.* 173, 479–485. <https://doi.org/10.2113/173.5.479>

485 Coynel, A., Blanc, G., Marache, A., Schäfer, J., Dabrin, A., Maneux, E., Bossy, C., Masson,
486 M., Lavaux, G., 2009. Assessment of metal contamination in a small mining- and smelting-
487 affected watershed: high resolution monitoring coupled with spatial analysis by GIS. *J.*
488 *Environ. Monit.* 11, 962–976. <https://doi.org/10.1039/B818671E>

489 Coynel, A., Schäfer, J., Dabrin, A., Girardot, N., Blanc, G., 2007. Groundwater contributions
490 to metal transport in a small river affected by mining and smelting waste. *Water Res.* 41,
491 3420–3428. <https://doi.org/10.1016/j.watres.2007.04.019>

492 Dabrin, A., Schäfer, J., Blanc, G., Strady, E., Masson, M., Bossy, C., Castelle, S., Girardot,
493 N., Coynel, A., 2009. Improving estuarine net flux estimates for dissolved cadmium export at
494 the annual timescale: Application to the Gironde Estuary. *Estuar. Coast. Shelf Sci.* 84, 429–
495 439. <https://doi.org/10.1016/j.ecss.2009.07.006>

496 Daskalakis, K.D., O'Connor, T.P., 1995. Normalization and Elemental Sediment
497 Contamination in the Coastal United States. *Environ. Sci. Technol.* 29, 470–477.
498 <https://doi.org/10.1021/es00002a024>

499 de Gramont, X., Braux, C., 1990. Synthèse Sud Limousin (No. R 31814 DEX-DAM-90),
500 Inventaire des ressources minières du territoire métropolitain. BRGM, Aubière.

501 El Hadri, H., Chéry, P., Jalabert, S., Lee, A., Potin-Gautier, M., Lespes, G., 2012. Assessment
502 of diffuse contamination of agricultural soil by copper in Aquitaine region by using French
503 national databases. *Sci. Total Environ.* 441, 239–247.
504 <https://doi.org/10.1016/j.scitotenv.2012.09.070>

505 Esri, 2012. ArcGIS Desktop. Environmental Systems Research Institute, Redlands.

506 Facchinelli, A., Sacchi, E., Mallen, L., 2001. Multivariate statistical and GIS-based approach
507 to identify heavy metal sources in soils. *Environ. Pollut.* 114, 313–324.

508 Farnham, I.M., Singh, A.K., Stetzenbach, K.J., Johannesson, K.H., 2002. Treatment of
509 nondetects in multivariate analysis of groundwater geochemistry data. *Chemom. Intell. Lab.*
510 *Syst.* 60, 265–281. [https://doi.org/10.1016/S0169-7439\(01\)00201-5](https://doi.org/10.1016/S0169-7439(01)00201-5)

511 GIS Sol, 2011. L'état des sols de France. Groupement d'intérêt scientifique sur les sols.

512 Grosbois, C., Courtin-Nomade, A., Martin, F., Bril, H., 2007. Transportation and evolution of
513 trace element bearing phases in stream sediments in a mining – Influenced basin (Upper Isle
514 River, France). *Appl. Geochem.* 22, 2362–2374.
515 <https://doi.org/10.1016/j.apgeochem.2007.05.006>

516 Hickey, M.G., Kittrick, J.A., 1984. Chemical Partitioning of Cadmium, Copper, Nickel and
517 Zinc in Soils and Sediments Containing High Levels of Heavy Metals. *J. Environ. Qual.* 13,
518 372–376. <https://doi.org/10.2134/jeq1984.00472425001300030010x>

519 Hou, D., O'Connor, D., Nathanail, P., Tian, L., Ma, Y., 2017. Integrated GIS and multivariate
520 statistical analysis for regional scale assessment of heavy metal soil contamination: A critical
521 review. *Environ. Pollut.* 231, 1188–1200. <https://doi.org/10.1016/j.envpol.2017.07.021>

522 IARC, 1993. Beryllium, cadmium, mercury, and exposures in the glass manufacturing
523 industry: views and expert opinions of an IARC Working Group on the Evaluation of
524 Carcinogenic Risks to Humans, which met in Lyon, 9 - 16 February 1993, IARC monographs
525 on the evaluation of carcinogenic risks to humans. Lyon.

526 [dataset] INRA, 2018. Base de Données Géographique des Sols de France à 1/1 000 000
527 version 3.2.8.0, 10/09/1998. Portail Data INRAE, V1. <https://doi.org/10.15454/BPN57S>

528 Jolivet, C., Boulonne, L., Ratié, C., 2006. Manuel du Réseau de mesures de la qualité des
529 sols, édition 2006. INRA, US 1106 InfoSol, Orléans.

530 Kierczak, J., Neel, C., Bril, H., Puziewicz, J., 2007. Effect of mineralogy and pedoclimatic
531 variations on Ni and Cr distribution in serpentine soils under temperate climate. *Geoderma*
532 142, 165–177. <https://doi.org/10.1016/j.geoderma.2007.08.009>

533 Lê, S., Josse, J., Husson, F., 2008. FactoMineR : An R Package for Multivariate Analysis. *J.*
534 *Stat. Softw.* 25, 1–18. <https://doi.org/10.18637/jss.v025.i01>

535 Lerat-Hardy, A., Coynel, A., Dutruch, L., Pereto, C., Bossy, C., Gil-Diaz, T., Capdeville, M.-
536 J., Blanc, G., Schäfer, J., 2019. Rare Earth Element fluxes over 15 years into a major
537 European Estuary (Garonne-Gironde, SW France): Hospital effluents as a source of
538 increasing gadolinium anomalies. *Sci. Total Environ.* 656, 409–420.
539 <https://doi.org/10.1016/j.scitotenv.2018.11.343>

540 Mamindy-Pajany, Y., Sayen, S., Guillon, E., 2013. Impact of sewage sludge spreading on
541 nickel mobility in a calcareous soil: adsorption–desorption through column experiments.
542 *Environ. Sci. Pollut. Res.* 20, 4414–4423. <https://doi.org/10.1007/s11356-012-1357-3>

- 543 Mandal, B., 2002. Arsenic round the world: a review. *Talanta* 58, 201–235.
544 [https://doi.org/10.1016/S0039-9140\(02\)00268-0](https://doi.org/10.1016/S0039-9140(02)00268-0)
- 545 Marchant, B.P., Saby, N.P.A., Arrouays, D., 2017. A survey of topsoil arsenic and mercury
546 concentrations across France. *Chemosphere* 181, 635–644.
547 <https://doi.org/10.1016/j.chemosphere.2017.04.106>
- 548 Marchant, B.P., Saby, N.P.A., Lark, R.M., Bellamy, P.H., Jolivet, C.C., Arrouays, D., 2010.
549 Robust analysis of soil properties at the national scale: cadmium content of French soils. *Eur.*
550 *J. Soil Sci.* 61, 144–152. <https://doi.org/10.1111/j.1365-2389.2009.01212.x>
- 551 Martin-Garin, A., Gaudet, J.P., Charlet, L., Vitart, X., 2002. A dynamic study of the sorption
552 and the transport processes of cadmium in calcareous sandy soils. *Waste Manag.* 22, 201–
553 207. [https://doi.org/10.1016/S0956-053X\(01\)00070-8](https://doi.org/10.1016/S0956-053X(01)00070-8)
- 554 McGrath, S.P., Loveland, P.J., 1992. The soil geochemical atlas of England and Wales.
555 Blackie Academic & Professional, Glasgow.
- 556 McLaughlin, M.J., Parker, D.R., Clarke, J.M., 1999. Metals and micronutrients – food safety
557 issues. *Field Crops Res.* 60, 143–163. [https://doi.org/10.1016/S0378-4290\(98\)00137-3](https://doi.org/10.1016/S0378-4290(98)00137-3)
- 558 Mellor, A., McCartney, C., 1994. The effects of lead shot deposition on soils and crops at a
559 clay pigeon shooting site in northern England. *Soil Use Manag.* 10, 124–129.
560 <https://doi.org/10.1111/j.1475-2743.1994.tb00472.x>
- 561 Morvan, X., Saby, N.P.A., Arrouays, D., Le Bas, C., Jones, R.J.A., Verheijen, F.G.A.,
562 Bellamy, P.H., Stephens, M., Kibblewhite, M.G., 2008. Soil monitoring in Europe: A review
563 of existing systems and requirements for harmonisation. *Sci. Total Environ.* 391, 1–12.
564 <https://doi.org/10.1016/j.scitotenv.2007.10.046>
- 565 Navarro-Pedreño, J., Almendro-Candel, M.B., Jordan-Vidal, M.M., Mataix-Solera, J., Garcia-
566 Sanchez, E., 2003. Mobility of cadmium, chromium, and nickel through the profile of a
567 calcisol treated with sewage sludge in the southeast of Spain. *Environ. Geol.* 44, 545–553.
568 <https://doi.org/10.1007/s00254-003-0790-5>
- 569 Orgiazzi, A., Ballabio, C., Panagos, P., Jones, A., Fernández-Ugalde, O., 2018. LUCAS Soil,
570 the largest expandable soil dataset for Europe: a review. *European Journal of Soil Science* 69,
571 140–153. <https://doi.org/10.1111/ejss.12499>
- 572 Papadopoulos, P., Rowell, D.L., 1988. The reactions of cadmium with calcium carbonate
573 surfaces. *J. Soil Sci.* 39, 23–36. <https://doi.org/10.1111/j.1365-2389.1988.tb01191.x>
- 574 Pebesma, E.J., 2004. Multivariable geostatistics in S: the gstat package. *Comput. Geosci.* 30,
575 683–691. <https://doi.org/10.1016/j.cageo.2004.03.012>
- 576 Pougnet, F., Blanc, G., Mulamba-Guilhemat, E., Coynel, A., Gil-Diaz, T., Bossy, C., Strady,
577 E., Schäfer, J., 2019. Nouveau modèle analytique pour une meilleure estimation des flux nets
578 annuels en métaux dissous. Cas du cadmium dans l'estuaire de la Gironde. *Hydroécologie*
579 *Appliquée*. <https://doi.org/10.1051/hydro/2019002>
- 580 R Core Team, 2019. R: A language and environment for statistical computing. R Foundation
581 for Statistical Computing, Vienna, Austria.
- 582 Ranjard, L., Nowak, V., Echairi, A., Faloya, V., Chaussod, R., 2008. The dynamics of soil
583 bacterial community structure in response to yearly repeated agricultural copper treatments.
584 *Res. Microbiol.* 159, 251–254. <https://doi.org/10.1016/j.resmic.2008.02.004>

585 Redon, P.-O., Bur, T., Guisresse, M., Probst, J.-L., Toiser, A., Revel, J.-C., Jolivet, C., Probst,
586 A., 2013. Modelling trace metal background to evaluate anthropogenic contamination in
587 arable soils of south-western France. *Geoderma* 206, 112–122.
588 <https://doi.org/10.1016/j.geoderma.2013.04.023>

589 Reimann, C., Filzmoser, P., Garrett, R.G., 2005. Background and threshold: critical
590 comparison of methods of determination. *Sci. Total Environ.* 346, 1–16.
591 <https://doi.org/10.1016/j.scitotenv.2004.11.023>

592 Righi, D., Wilbert, J., 1984. Les sols sableux podzolisés des Landes de Gascogne (France):
593 répartition et caractères principaux. *Science du sol*, 253–264.

594 Rooney, C.P., Zhao, F.-J., McGrath, S.P., 2007. Phytotoxicity of nickel in a range of
595 European soils: Influence of soil properties, Ni solubility and speciation. *Environ. Pollut.* 145,
596 596–605. <https://doi.org/10.1016/j.envpol.2006.04.008>

597 Saby, N., Arrouays, D., Boulonne, L., Jolivet, C., Pochot, A., 2006. Geostatistical assessment
598 of Pb in soil around Paris, France. *Sci. Total Environ.* 367, 212–221.
599 <https://doi.org/10.1016/j.scitotenv.2005.11.028>

600 [dataset] Saby, N., Bertouy, B., Boulonne, L., Bispo, A., Ratié, C., Jolivet, C., 2019.
601 Statistiques sommaires issues du RMQS sur les données agronomiques et en éléments traces
602 des sols français de 0 à 50 cm. Portail Data INRAE, V5. <https://doi.org/10.15454/BNCXYB>

603 Saby, N., Marchant, B.P., Lark, R.M., Jolivet, C.C., Arrouays, D., 2011. Robust geostatistical
604 prediction of trace elements across France. *Geoderma* 162, 303–311.
605 <https://doi.org/10.1016/j.geoderma.2011.03.001>

606 Saby, N., Thioulouse, J., Jolivet, C.C., Ratié, C., Boulonne, L., Bispo, A., Arrouays, D., 2009.
607 Multivariate analysis of the spatial patterns of 8 trace elements using the French soil
608 monitoring network data. *Sci. Total Environ.* 407, 5644–5652.
609 <https://doi.org/10.1016/j.scitotenv.2009.07.002>

610 Salminen, R., 2005. Geochemical atlas of Europe Pt. 1. Background information,
611 methodology and maps. Geological Survey of Finland, Espoo.

612 Salpeteur, I., Maldan, F., 2011. French geochemical baseline data for trace elements in top-
613 and bottom-soils and overbanks of the shield areas and sediment covers: A low density survey
614 in the FOREGS Geochemical Atlas of Europe (II). *Environ. Risques Santé* 299–315.
615 <https://doi.org/10.1684/ers.2011.0479>

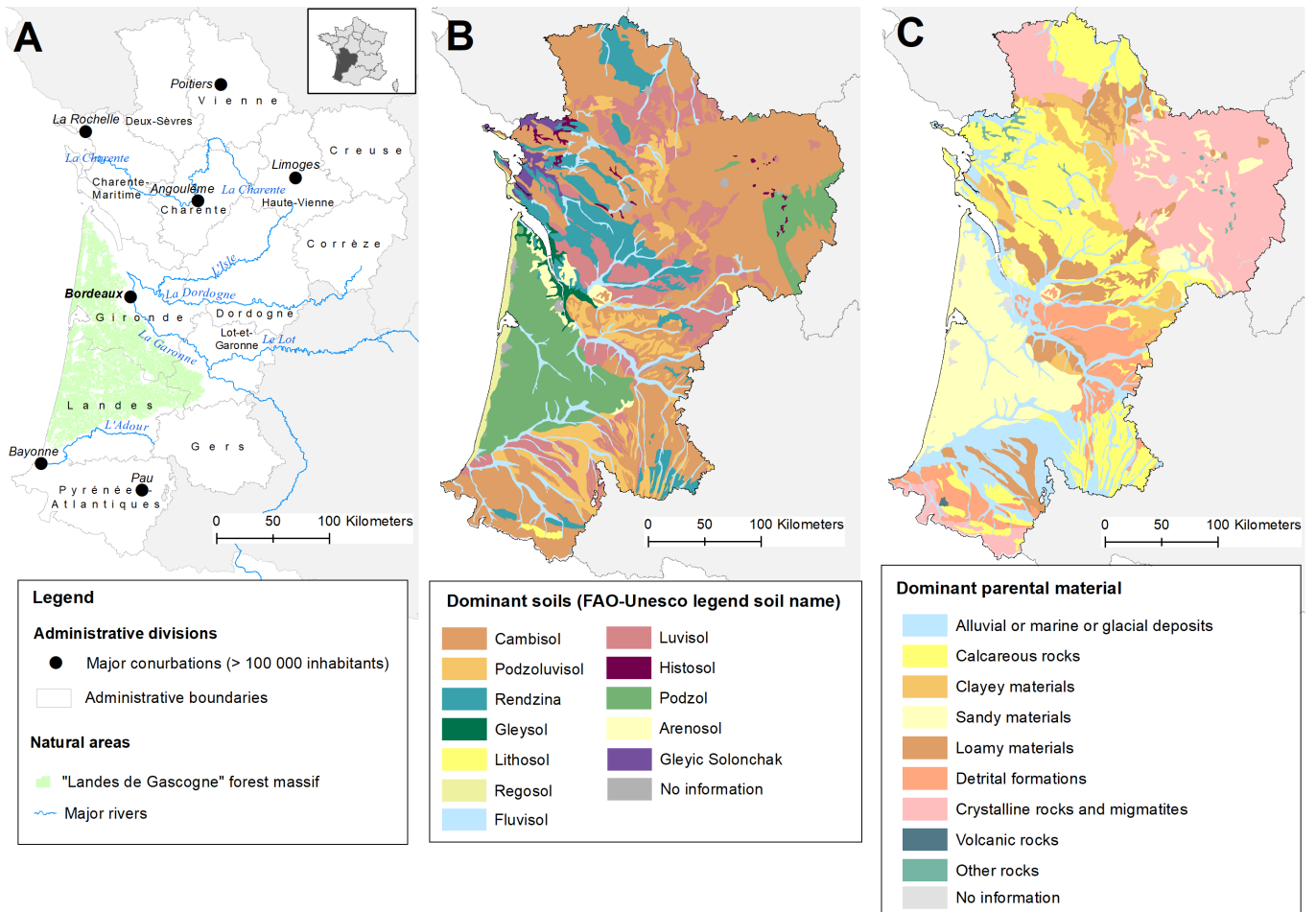
616 Schäfer, J., Hannker, D., Eckhardt, J.-D., Stüben, D., 1998. Uptake of traffic-related heavy
617 metals and platinum group elements (PGE) by plants. *Sci. Total Environ.* 215, 59–67.
618 [https://doi.org/10.1016/S0048-9697\(98\)00115-6](https://doi.org/10.1016/S0048-9697(98)00115-6)

619 Schiff, K.C., Weisberg, S.B., 1999. Iron as a reference element for determining trace metal
620 enrichment in Southern California coastal shelf sediments. *Mar. Environ. Res.* 48, 161–176.
621 [https://doi.org/10.1016/S0141-1136\(99\)00033-1](https://doi.org/10.1016/S0141-1136(99)00033-1)

622 Senesil, G.S., Baldassarre, G., Senesi, N., Radina, B., 1999. Trace element inputs into soils by
623 anthropogenic activities and implications for human health. *Chemosphere, Matter and Energy*
624 *Fluxes in the Anthropocentric Environment* 39, 343–377. [https://doi.org/10.1016/S0045-](https://doi.org/10.1016/S0045-6535(99)00115-0)
625 [6535\(99\)00115-0](https://doi.org/10.1016/S0045-6535(99)00115-0)

626 Shacklette, H.T., Boerngen, J.G., 1984. Element concentrations in soils and other surficial
627 materials of the conterminous United States. USGS Professional Paper 1270.

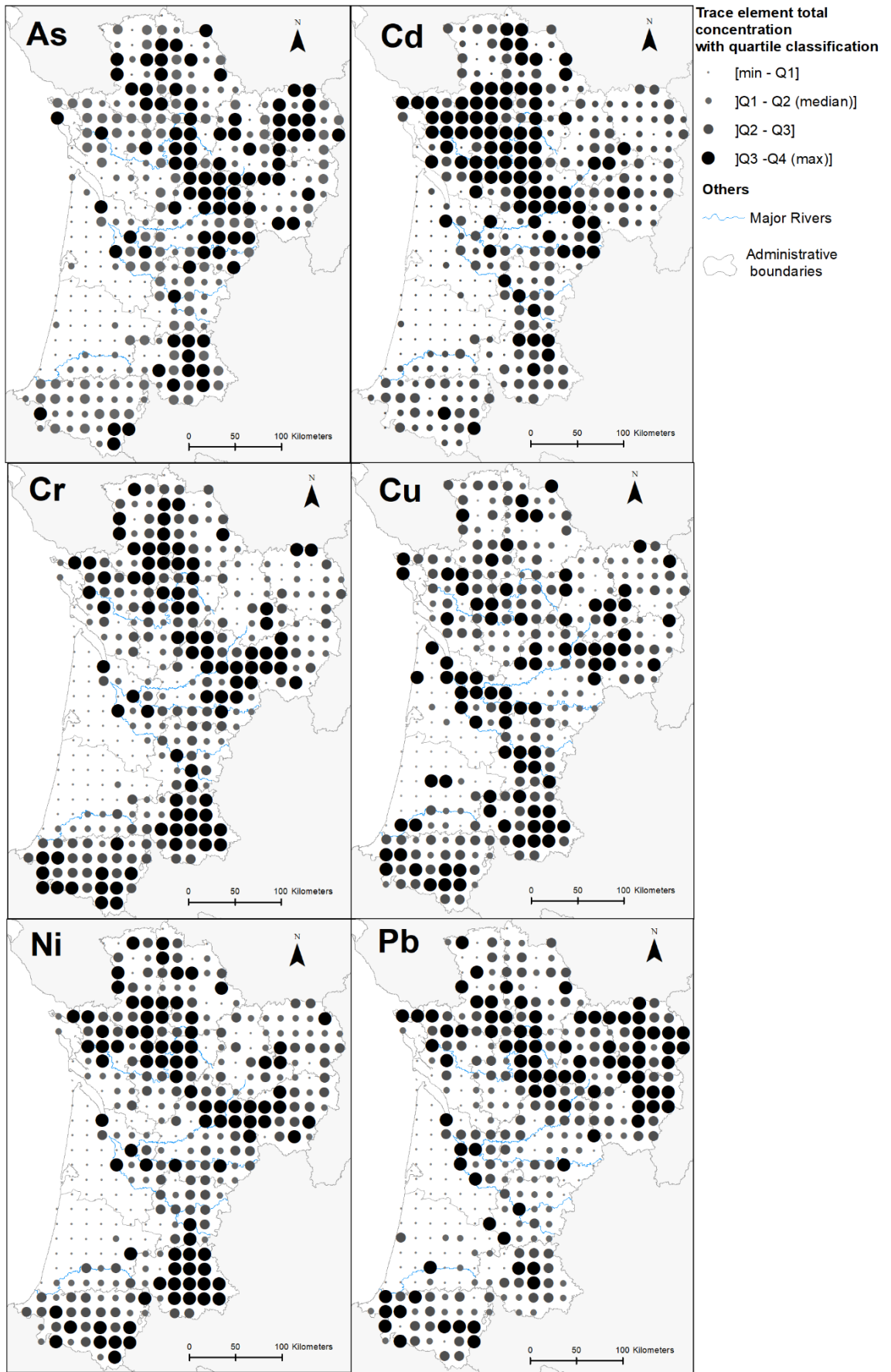
- 628 Tsuji, L.J.S., Karagatzides, J.D., 1998. Spent lead shot in the western James Bay region of
629 northern Ontario, Canada: Soil and plant chemistry of a heavily hunted wetland. *Wetlands* 18,
630 266–271. <https://doi.org/10.1007/BF03161662>
- 631 Tukey, J.W., 1977. *Exploratory data analysis*, Addison-Wesley series in behavioral science :
632 quantitative methods. Addison-Wesley, Reading.
- 633 Villanneau, E., Perry-Giraud, C., Saby, N., Jolivet, C., Marot, F., Maton, D., Floch-Barneaud,
634 A., Antoni, V., Arrouays, D., 2008. Détection de valeurs anomaliques d'éléments traces
635 métalliques dans les sols à l'aide du Réseau de Mesure de la Qualité des Sols. *Etude et*
636 *Gestion des sols* 15, 183–200.
- 637 Webster, R., Oliver, M.A., 1993. How large a sample is needed to estimate the regional
638 variogram adequately?, in: Soares, A. (Ed.), *Geostatistics Tróia '92: Volume 1, Quantitative*
639 *Geology and Geostatistics*. Springer Netherlands, Dordrecht, pp. 155–166.
640 https://doi.org/10.1007/978-94-011-1739-5_14
- 641 Zehetner, F., Rosenfellner, U., Mentler, A., Gerzabek, M.H., 2009. Distribution of Road Salt
642 Residues, Heavy Metals and Polycyclic Aromatic Hydrocarbons across a Highway-Forest
643 Interface. *Water. Air. Soil Pollut.* 198, 125–132. <https://doi.org/10.1007/s11270-008-9831-8>



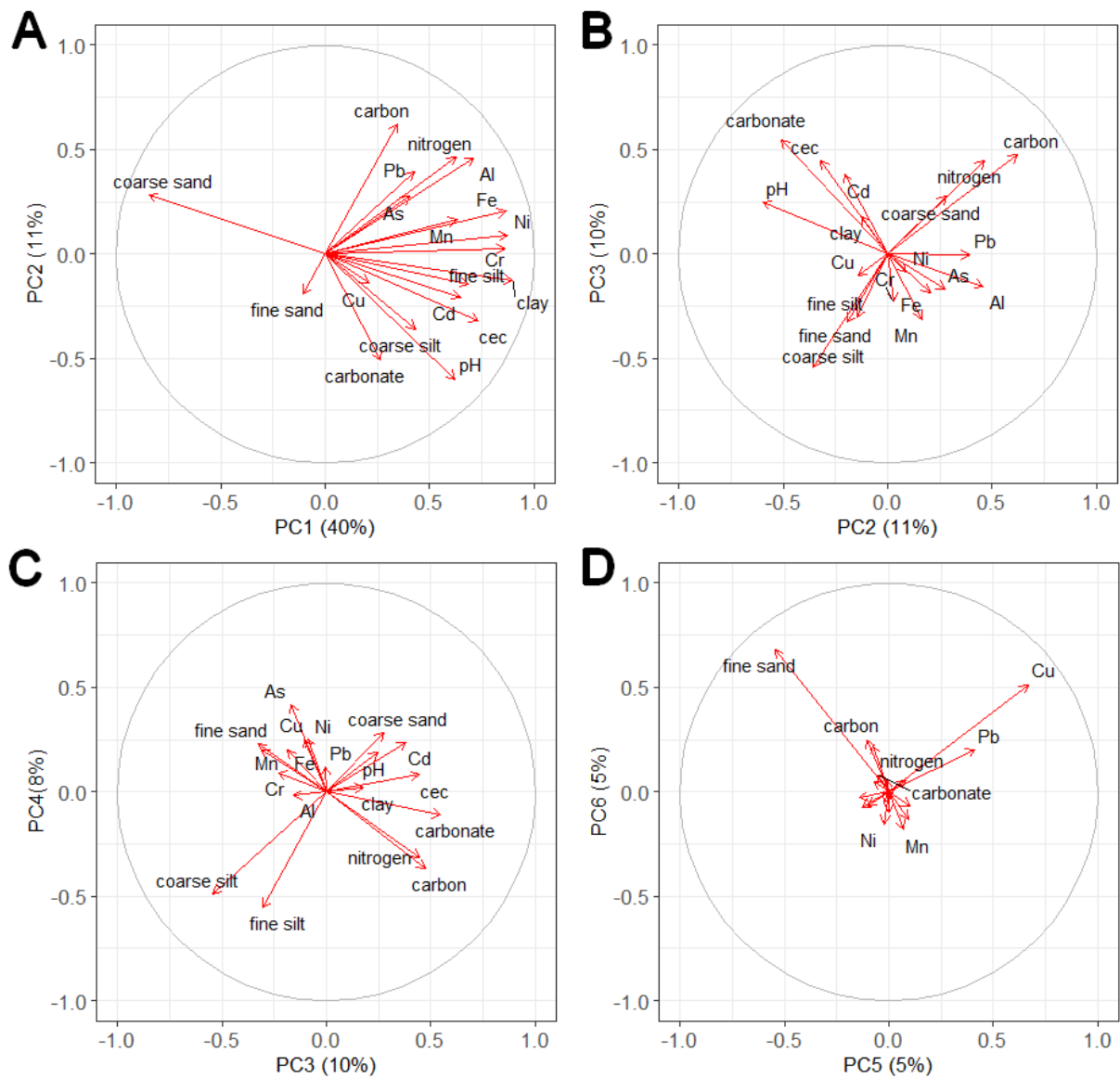
644

645 Figure 1: A) Map describing the administrative divisions of the study area and major natural areas. B) Map
 646 of dominant soils from the Soil Geographical Data Base of France (BDGSF) at scale 1:1000000 (INRA,
 647 2018). C) Map of the dominant parent material from the BDGSF.

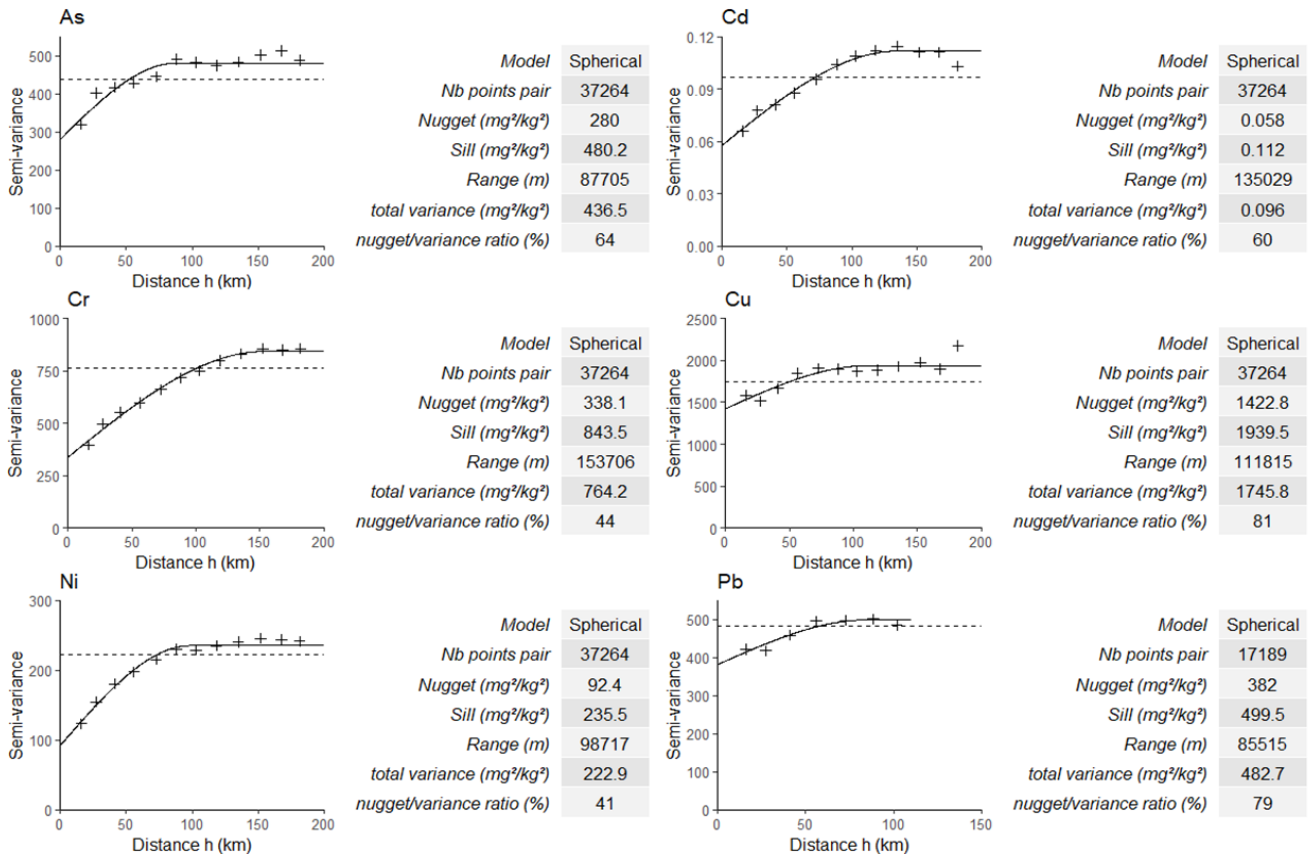
648



649 Figure 2: Point distribution of As, Cd, Cr, Cu, Ni and Pb concentrations with classification by quartile in
 650 the topsoil of southwestern France.

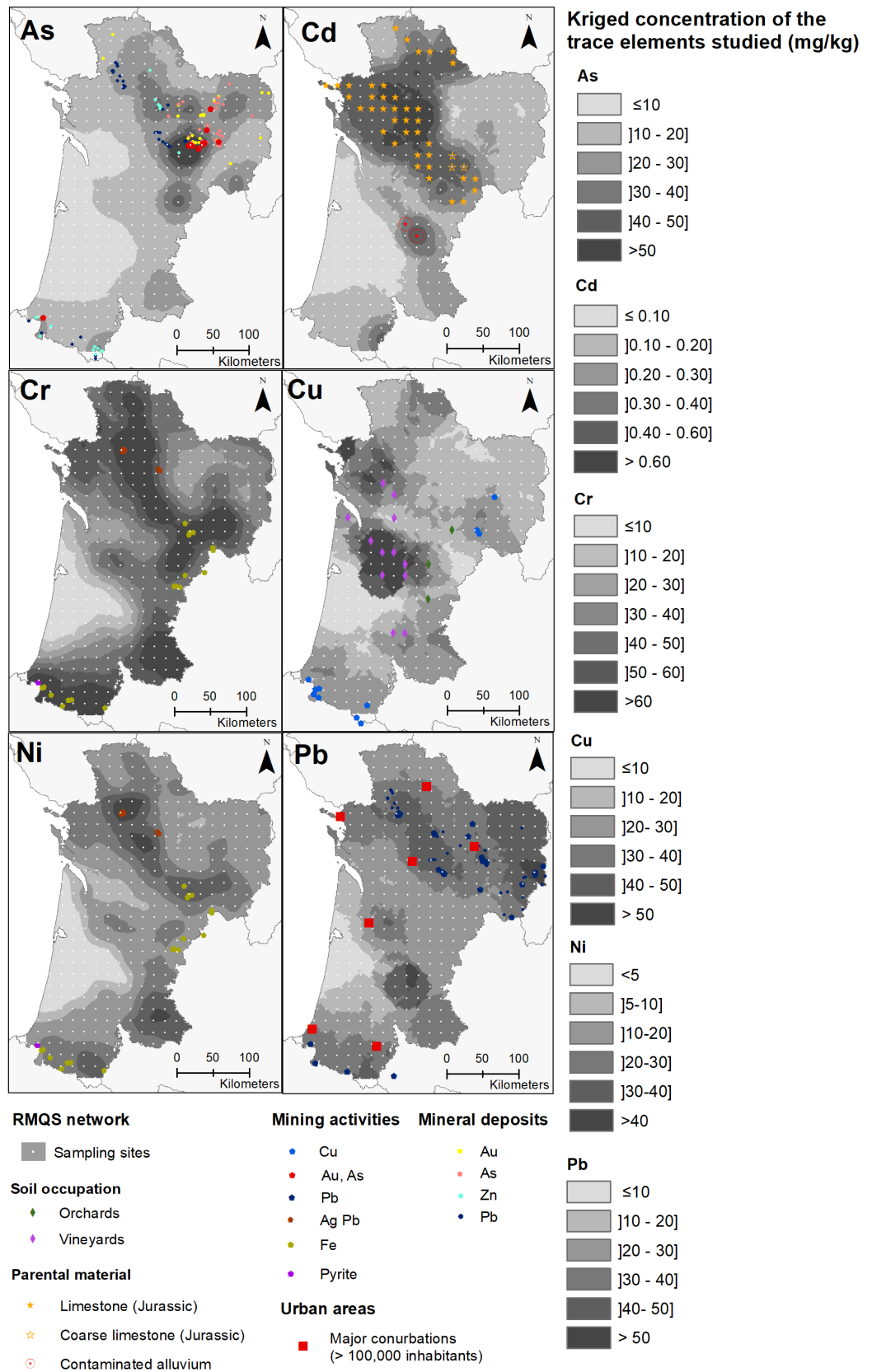


651 Figure 3: Variable factor maps of the principal components analysis. On each axis, in bracket,
 652 the percentage of variance explained by the principal components (PC). A) PC 1 and PC 2; B)
 653 PC 2 and PC 3; C) PC 3 and 4 D) PC 5 and PC 6.



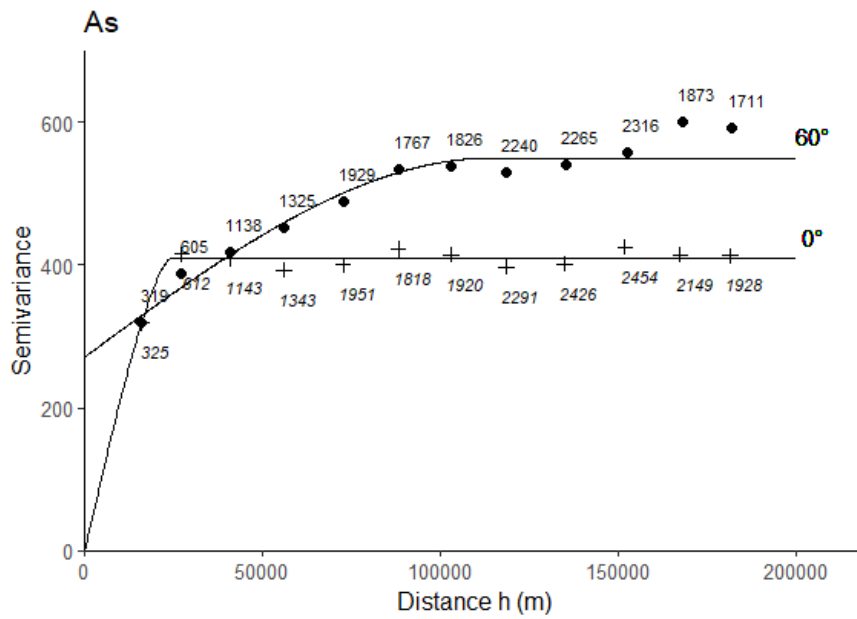
655

656 Figure 4: Omnidirectional semivariograms, experimental (cross), and fitted with spherical model
 657 (black line). Dashed line corresponds to the total variance. Pb experimental semivariogram is cut
 658 from 100,000 meters because the semivariance decreases sharply after this distance. The data at the
 659 top right of each graph describe the modeled semivariograms. For each semivariogram the number
 660 (nb) of points pair is superior to 50 (Webster and Oliver, 1993).



661
662
663
664
665
666
667

Figure 5: Maps with kriged concentrations of studied trace elements, and geographic information describing soil occupation, geology, mineral deposits and mining activities over the SWF. Soil occupation and geological data are shown on maps over sampling sites and originate from site description and geological maps, respectively (BRGM, 2005). Mineral deposits and mining activities data are shown on the maps at their exact location (BRGM, 2007).



Angle (degrees)	0	60
Model	Circular	Spherical
Nb points pair	20360	19314
Nugget (mg ² /kg ²)	0.0	271.5
Sill (mg ² /kg ²)	408.7	549.9
Range (m)	24014	114652

668

669

670 Figure 6: Directional semivariograms of As. Crosses represent 0° semivariance data, dots represent
 671 60° semivariance data. For each semivariance value, the number of point pair is shown. The solid lines
 672 represent the modeled semivariograms, with their descriptive parameters to the right of the figure.
 673

674 Table 1: Descriptive statistics of As, Cd, Cr, Cu, Ni and Pb total concentrations in soils (in mg/kg) and
 675 assessment of anomalous values at regional and *national* scales (Saby et al., 2019). Regional values
 676 are included in the national dataset.

	As	Cd	Cr	Cu	Ni	Pb
Number of values (national)	2130	2144	2144	2144	2144	2144
Number of values (region)	356	356	356	356	356	356
Minimum (region)	0.39	0.01	1	0.5	0.5	3.1
Maximum (region)	209	2.1	168	491	73.6	261
1st quartile (region)	7.8	0.06	20.8	6.0	6.5	19
Median (region)	13.1	0.15	44	13.1	14.9	27.1
<i>Median (national)</i>	<i>12.0</i>	<i>0.20</i>	<i>53.2</i>	<i>13.9</i>	<i>19.3</i>	<i>27.8</i>
3rd quartile (region)	20.8	0.28	60.0	22.9	27.9	37.9
Regional upper whisker	41.2	0.60	118.6	48.3	60.0	66.3
<i>National upper whisker</i>	<i>36.7</i>	<i>0.65</i>	<i>121.7</i>	<i>42.8</i>	<i>61.5</i>	<i>62.0</i>
Number of values (region) > regional upper whisker	25	40	6	36	7	16
<i>Number of values (region) > national upper whisker</i>	<i>30</i>	<i>35</i>	<i>4</i>	<i>42</i>	<i>5</i>	<i>23</i>

677 Table 2: Descriptive statistics of granulometry, pH, CaCO₃, carbon, nitrogen, total Al, Fe and
 678 Mn of the 356 soil samples.
 679

Variable	<i>unit</i>	Min	1st quartile	Median	3rd quartile	Max
Clay	%	0.2	12.58	19.75	32.3	65.2
Fine silt	%	0.1	12.43	19.25	26.53	45.3
Coarse silt	%	0.1	6.7	11.05	16.6	38.6
Fine sand	%	0.5	8.28	12	16.13	59.8
Coarse sand	%	0.6	10.83	23.85	49.15	97
CaCO ₃	<i>g/kg</i>	0.5	0.5	0.5	2.05	706
pH		4	4.9	5.8	7.4	8.4
CEC	<i>cmolc/kg</i>	0.25	3.84	6.61	17.33	50.6
Organic carbon	%	0.059	1.22	1.73	2.68	13.4
Total nitrogen	‰	0.03	0.94	1.50	2.3	9.79
Al	%	0.12	2.52	4.44	6.66	10.2
Fe	%	0.03	1.08	2.17	3.14	7.66
Mn	<i>mg/kg</i>	5	195.8	485.5	738.5	4870

680
 681

693 Table S1: Contribution of variables to each dimension of the PCA (%). The highest contributions
 694 (>5.3%) are in bold.

Variables	PC 1	PC 2	PC 3	PC 4	PC 5	PC 6
clay	10.52	0.72	1.57	0.03	0.00001	0.93
fine silt	6.17	0.96	4.61	21.54	1.00	0.51
coarse silt	2.45	5.89	14.87	16.78	0.61	0.29
fine sand	0.14	1.68	5.38	3.69	29.26	46.64
coarse sand	9.30	3.60	3.78	5.59	0.86	1.72
cec	7.03	4.69	10.07	0.47	0.01	0.11
pH	5.05	16.47	3.09	2.42	0.01	0.33
carbonate (CaCO ₃)	0.92	11.85	15.10	0.84	0.29	0.65
carbon	1.57	17.64	11.37	9.48	1.04	6.21
nitrogen	5.09	9.83	10.03	6.89	0.61	4.87
Fe	9.79	1.90	1.75	2.78	1.58	0.54
Mn	5.21	1.24	4.91	2.89	0.48	3.30
Cd	5.46	1.98	7.26	3.95	0.05	0.24
Al	6.60	9.66	1.23	0.02	0.49	0.25
Cu	0.58	0.91	0.55	4.37	44.10	26.41
Pb	2.35	7.12	0.00	0.95	16.59	4.09
As	2.13	3.46	1.43	12.21	1.92	0.08
Ni	9.97	0.38	0.40	4.52	0.06	2.38
Cr	9.68	0.03	2.59	0.59	1.03	0.45

695